Article

Conduction Properties of Bipyridinium-Functionalized Molecular Wires

Alexei Bagrets, Andreas Arnold, and Ferdinand Evers

J. Am. Chem. Soc., **2008**, 130 (28), 9013-9018 • DOI: 10.1021/ja800459k • Publication Date (Web): 21 June 2008

J|A|C|S
ARTICLES

Published on Web 06/21/2008

Conduction Properties of Bipyridinium-Functionalized Molecular Wires

Alexei Bagrets,*[,†,‡] Andreas Arnold,[†] and Ferdinand Evers*[,†,‡]

Institut für Theorie der Kondensierten Materie, Universität Karlsruhe, D-76128 Karlsruhe, Germany, and Institute of Nanotechnology, Research Center Karlsruhe, P.O. Box 3640, D-76021, Germany

Received January 30, 2008; E-mail: alexej.bagrets@int.fzk.de; ferdinand.evers@int.fzk.de

Abstract: We present a detailed analysis of the coherent electron transport through a redox-active, 4,4′-bipyridinium (viologen)-functionalized molecular wire, which was studied in several recent experiments. Our calculations for the bare viologen predict conductances differing by 2 orders of magnitude depending on the contact geometry. For the alkyl-wired viologen unit, we obtain an exponential decay of the conductance with the wire length. Because this exponent also governs the conductance in the incoherent transport regime, comparison with experiments is legitimate and we find a good agreement. Furthermore, our calculations indicate that the experimentally observed conductance switching behavior is not amenable to an explanation inside a coherent transport picture. A possible incoherent mechanism is being discussed.

Introduction

Integration of molecular structures as active components in electronic circuits[1] is the visionary concept underlying molecular electronics and, simultaneously, a scientific challenge. The ongoing progress in the development of experimental tools, including, for example, scanning tunneling microscopy (STM), or nanolithography and -pattering techniques, makes it possible to contact a single or few molecules to macroscopic electrodes to explore electron charge transfer. Thus, the current−voltage characteristics can be measured through molecules trapped within electromigrated junctions,[2] in mechanically controlled break-junctions,[3] or by use of an STM tip operating on a self-assembled molecular monolayer.[4–8]

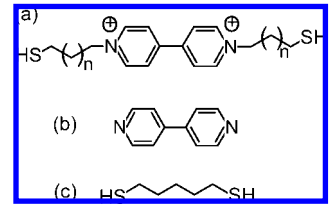

Figure 1. Molecules considered in this Article: (a) dithiolalkyl-viologens (nVn) comprising the central redox-active unit (viologen); (b) 4,4′-bipyridine; and (c) alkanedithiols.

On the way to functional molecular units, 4,4′-bipyridine (44BP, see Figure 1) looks promising as a candidate for the realization of a molecular switch. The two pyridyl rings form two separate π-conjugated subsystems, coupled via a C−C bond. The steric interaction between hydrogen atoms of neighboring rings forces the charge neutral 44BP to have a torsion angle around 35°. If additional electrons are added, the C−C bond length increases by ∼5%. This suffices to reduce the steric effect, so that the molecule flips into a flat conformation, where electrons of both pyridyl units form a common, conjugated π-system (Hückel's rule[9]). Because the flat conformation supports extended states, one could expect an increase in the molecular conductance and, hence, a "flip–flop" switching behavior. Indeed, adding and removing of electrons is experimentally feasible, for example, by applying a gate voltage electrochemically.

Transport properties of 44BP have been addressed experimentally by Xu and Tao.[4] Simultaneously with repeated formation and breaking of the Au–molecule–Au junctions, hundreds of current–distance traces were measured. Statistical information was collected in conductance histograms, which

† Universität Karlsruhe.
‡ Research Center Karlsruhe.

(1) (a) Joachim, C.; Gimezewski, J. K.; Aviram, A. *Nature* **2000**, *408*, 541–548. (b) Chen, Y.; Jung, G.-Y.; Ohlberg, D. A. A.; Li, X.; Stewart, D. R.; Jeppesen, J. O.; Nielsen, K. A.; Stoddart, J. F.; Williams, R. S. *Nanotechnology* **2003**, *14*, 462–468. (c) Liao, J.; Bernard, L.; Langer, M.; Schönenberger, C.; Calame, M. *Adv. Mater.* **2006**, *18*, 2444–2447. (d) Guo, X.; Whalley, A.; Klare, J. E.; Huang, L.; OBrien, S.; Steigerwald, M.; Nuckolls, C. *Nano Lett.* **2007**, *7*, 1119–1122.
(2) (a) Park, H.; Park, J.; Lim, A. K. L.; Anderson, E. H.; Alivisatos, A. P.; McEuen, P. L. *Nature* **2000**, *407*, 57–60. (b) Park, J.; Pasupathy, A. N.; Goldsmith, J. I.; Chang, C.; Yaish, Y.; Petta, J. R.; Rinkoski, M.; Sethna, J. P.; Abruna, H. D.; McEuen, P. L.; Ralph, D. C. *Nature* **2002**, *417*, 722–725. (c) Yu, L. H.; Keane, Z. K.; Ciszek, J. W.; Cheng, L.; Stewart, M. P.; Tour, J. M.; Natelson, D. *Phys. Rev. Lett.* **2004**, *93*, 266802–4.
(3) (a) Reichert, J.; Ochs, R.; Beckmann, D.; Weber, H. B.; Mayor, M.; v. Löhneysen, H. *Phys. Rev. Lett.* **2002**, *88*, 176804-4. (b) Lörtscher, E.; Ciszek, J. W.; Tour, J.; Riel, H. *Small* **2006**, *8−9*, 973–977.
(4) Xu, B.; Tao, N. J. *Science* **2003**, *301*, 1221–1223.
(5) Haiss, W.; van Zalinge, H.; Higgins, S. J.; Bethell, D.; Höbenreich, H.; Schiffrin, D. J.; Nichols, R. J. *J. Am. Chem. Soc.* **2003**, *125*, 15294–15295.
(6) Jäckel, F.; Watson, M. D.; Müllen, K.; Rabe, J. P. *Phys. Rev. Lett.* **2004**, *92*, 188303.
(7) Li, Zh.; Pobelov, I.; Han, B.; Wandlowski, Th.; Błaszczyk, A.; Mayor, M. *Nanotechnology* **2007**, *18*, 044018-8.
(8) Xu, B.; Xiao, X.; Yang, X.; Zang, L.; Tao, N. *J. Am. Chem. Soc.* **2005**, *127*, 2386–2387.
(9) Gutman, I.; Trinajstić, N. *J. Chem. Phys.* **1976**, *64*, 4921–4925.

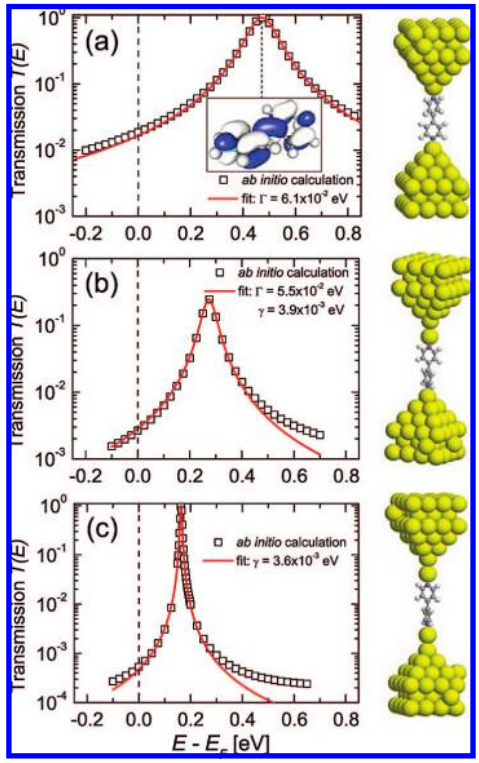

Figure 2. Transmission spectra of three typical configurations of 4,4′-bipyridine (44BP) coupled to Au electrodes illustrating the cases of (a) strong–strong, (b) strong–weak, and (c) weak–weak coupling. Inset of plot (a) shows the 4,4′-bipyridinium dication LUMO giving rise to the transmission resonance positioned above the Fermi energy. The "□" are calculated values, while solid red lines correspond to Lorentzian fits (see text for further details).

showed well-pronounced, equidistantly separated peaks, suggesting a conductance value of the individual molecule $\sim 0.01 G_0$ (here $G_0 = 2e^2/h = 77.5\ \mu$S).

The nitrogen−gold bond, which is likely to be established under experimental conditions, originates from N lone pairs overlapping with Au states. A much stronger, sulfur−gold coordination covalent bond forms with thiol-modified molecules. To make use of this and establish well-defined contacts, flexible thiol–alkyl linkers (Figure 1) anchoring a bipyridinium unit (viologen moiety) to gold electrodes can be introduced. This idea was explored by Gittins et al.[10] and Haiss et al.,[5] followed by later work of Li et al.,[7] who studied the conductance of molecular junctions formed with dithiolalkyl-viologens (see Figure 1a).

By electrochemical gating of molecular wires, the oxidation state of the central, reversibly reducible viologen (V) moiety could be controlled experimentally and driven from the dication V^{2+} to the radical cation state $V^{+\bullet}$. Switching indeed has been reported,[5,7] if only in a statistical sense, that is, for averaged conductances, with the values for the $V^{+\bullet}$ state being ∼50% larger[7] than that for V^{2+}. The effect was attributed to the already mentioned broken conjugation of the viologen dication in contrast to the conjugated radical cation.[5,7] Additional information was obtained varying alkyl chain length n (from 5 to 8, see Figure 1a). Measured conductances[7] showed a decaying tunneling law, $G_N \propto \exp(-\beta_{2n} N)$, with an exponent $\beta_{2n} \approx 0.75$ defined per number $N = 2n$ of methylene (CH_2) groups.

(10) Gittins, D. I.; Bethell, D.; Schiffrin, D. J.; Nichols, R. J. *Nature* **2000**, *408*, 67–69.

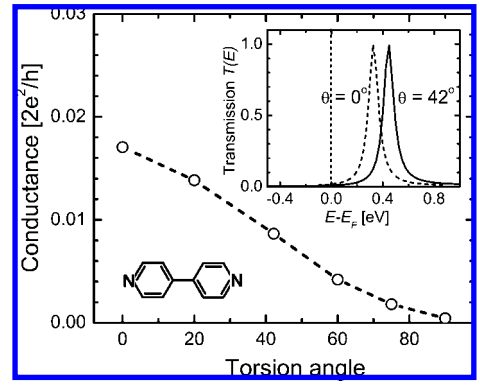

Figure 3. Conductance through a 44BP over a torsion angle θ between the pyridyl rings. Inset shows transmission around E_F for the planar molecule ($\theta = 0°$, - - -) and for the distorted one with the optimized angle $\theta = 42°$ (–).

Motivated by these experiments, we investigate in this Article the electron transport mechanisms through 44BP and its viologen derivatives (Figure 1), employing elaborate first-principle calculations. Our findings reveal the crucial role of atomistic details in the contact region that are specific to 44BP (Figure 2) and that can lead to conductance values differing by 2 orders of magnitude. Further, we show (Figure 4) that charge flow through viologen derivatives is governed by tunneling of electrons assisted by the LUMO localized at the redox-active bipyridinium unit. Our work does not lend support to the hypothesis that the "flip–flop" mechanism is the main switching agent[5,7] in viologens. Instead, inelastic transport may explain the observed switching behavior.

Method

Electronic structure calculations of 44BP, alkanedithiols, and viologen derivatives coupled to Au electrodes have been performed using the quantum chemistry package TURBOMOLE.[11] To simulate a contact region close to gold leads, calculations have been done for different conformations of the "extended molecule"

(11) (a) Treutler, O.; Ahlrichs, R. *J. Chem. Phys.* **1995**, *102*, 346–354. (b) Eichkorn, K.; Treutler, O.; Öhm, H.; Häser, M.; Ahlrichs, R. *Chem. Phys. Lett.* **1995**, *242*, 652–660. (c) Eichkorn, K.; Weigend, F.; Treutler, O.; Ahlrichs, R. *Theor. Chem. Acc.* **1997**, *97*, 119–124. (d) Sierka, M.; Hogekamp, A.; Ahlrichs, R. *J. Chem. Phys.* **2003**, *118*, 9136–9148.

(12) We employed the generalized gradient approximation (GGA, BP86 functional[13]) with the fully atom-optimized, contracted Gaussian-type basis set of triple-ζ valence quality including polarization functions (TZVP).[14] The lattice structure of Au clusters was chosen fcc with a lattice constant fixed to the experimental value 4.08 Å of bulk gold.

(13) (a) Becke, A. D. *Phys. Rev. A* **1988**, *38*, 3098–3100. (b) Perdew, J. P. *Phys. Rev. B* **1986**, *33*, 8822–8824.

(14) Schäfer, A.; Huber, C.; Ahlrichs, R. *J. Chem. Phys.* **1994**, *100*, 5829–5835.

(15) Evers, F.; Weigend, F.; Köntopp, M. *Phys. Rev. B* **2004**, *69*, 235411-9.

(16) (a) Evers, F.; Arnold, A. arXiv:cond-mat/0611401v1. (b) Arnold, A.; Weigend, F.; Evers, F. *J. Chem. Phys.* **2007**, *126*, 174101–14. (c) For an analytical derivation of the method, in the content of carbon nanotubes, see: Nemec, N.; Tomanek, D.; Cuniberti, G. arXiv: 0711.1088v1.

(17) We describe the interaction between the "extended molecule" and the rest of semi-infinite electrodes via an efficient approximation for the self-energy, represented by a local leakage function, $\Sigma(r, r') \approx i\eta\delta(r - r')$. To improve convergence with the number of Au contact atoms, we use chaotic cavities produced by adding a few adatoms to otherwise symmetric Au pyramids. The value of the level broadening η can then be varied by 1 order of magnitude (around ∼0.1 hartree in the present calculations) leaving the results for the transmission unchanged within a few percent.

composed of molecules bridging two pyramids of ~40÷55 Au atoms.[12] Relaxed conformations were found for the smaller molecular clusters comprising single Au atoms at each side, which then were placed between electrodes assuming different contact coordination geometries (see Figures 2,4a). Charge flow has been described within the nonequilibrium Green's function approach (NEGF) as implemented in our home-built simulation package.[15–17]

Theoretical Analysis

We start our discussion with analyzing conductance properties of 44BP. We show below that different geometrical arrangements in the contact region between the molecule and the electrodes can result in vastly different conductances. The 44BP has two lone pairs of electrons at each nitrogen atom. Because these lone pairs are not delocalized into the aromatic π-system, bipyridine can be protonated to form a twice positively charged ($Q = +2$) polyatomic ion–bipyridinium dication $[(C_5H_4NH)_2]^{2+}$ (44BP-dication), known as "viologen". Geometry optimization of the viologen revealed a dihedral angle of 42° between the pyridyl rings, with tilted structure having energy ~0.75 eV below the planar one. Considering the dication as a relevant reference molecule is motivated by the observation that in the break-junction geometry (see Figure 2) one of the equatorial nitrogen sp^2 orbitals hybridizes with neighboring Au s-states. In this process, a charge neutral 44BP donates an electron into the Au surface and forms a Au−N bond. Its length is found to be 2.05 Å.

Thus deprived of two electrons, transport properties are governed by the LUMO of 44BP-dication. This state is seen in the transmission function as a Lorentzian situated ~0.2÷0.5 eV above the Fermi energy (E_F), with a peak position E_{LUMO} being dependent on the exact arrangement of atoms in the contact region. Three typical examples are shown in Figure 2, where (001) oriented fcc electrodes were chosen. With a Lorentzian fit, $T(E) = \Gamma_L\Gamma_R/[(E - E_{LUMO})^2 + (\Gamma_L + \Gamma_R)^2/4]$, we have found that leakage rates $\Gamma_{L/R}$ can take either large values, $\Gamma \approx 5 \times 10^{-2}$ eV, or small ones, $\gamma \approx 5 \times 10^{-3}$ eV, depending on whether strong or weak coupling is realized. In case of strong coupling (Figure 2a), the tip gold atom, closest to nitrogen, has four neighboring Au atoms, $N_c = 4$, while in the case of weak coupling, $N_c = 1$ (see Figure 2c). A product of leakage rates determines the zero-bias conductance: $G \simeq G_0\Gamma_L\Gamma_R/(E_{LUMO} - E_F)$. Because of $\gamma/\Gamma \approx 0.1$, different contact configurations manifest themselves in conductances varying by orders of magnitude: values $1.9 \times 10^{-2}G_0$, $2.7 \times 10^{-3}G_0$, and $5.3 \times 10^{-4}G_0$ were obtained for cases (a), (b), and (c) in Figure 2, respectively.[18] We interpret the suppression of conductance in the case of weak coupling as being due to a reduced wave functions overlap between the LUMO with its extended π-system and the Au states.[22]

To address the conformational aspect of switching of 44BP, we have set different torsion angles θ and calculated conductances $G(\theta)$ (Figure 3). The transmission goes down with increasing θ, due to a gradual shift of the LUMO state upward in energy (inset of Figure 3). Access to this torsion degree of freedom can be and has been achieved by electrochemical gating.[5,7] However, in such experiments, switching is accompanied by (un)charging the molecule that implies an additional effect on the *I–V*, which we investigate in the following.

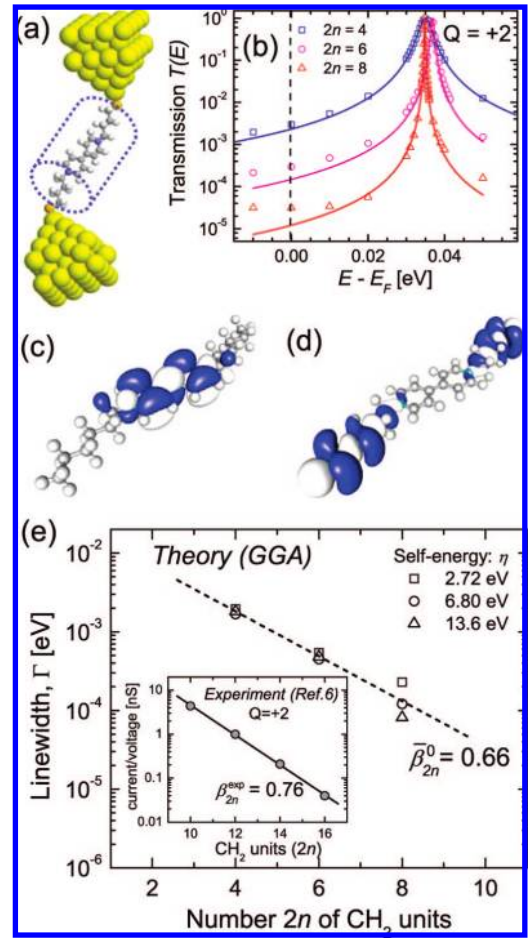

Figure 4. Resonant tunneling through dithiolalkyl-viologens (nVn, see Figure 1a): (a) Geometry of Au–nVn–Au junction together with the cylindrical gate screening a viologen charge;[25] (b) transmission through the molecular junctions around E_F with different alkyl spacer lengths n showing the dication-LUMO resonance; (c and d) molecular orbitals of the $n = 6$ alkyl-viologen: (c) is a redox-active $V^{+\bullet}$ HOMO state, while (d) is built of alkane HOMOs; (e) alkyl-wire length ($2n$) dependence of the resonance line width $\Gamma_n \propto \exp[-\bar{\beta}^0_{2n}(2n)]$ (symbols refer to different self-energy related parameters η showing convergence of results, see ref 17 for details); inset reproduces experimental data on the single molecule conductance reported by Li et al.,[7] where the current is defined by the line width: $I(V) \propto (e/h)\Gamma_n$.

Before examining the fully dressed viologen moiety shown in Figure 1a, we first recall the transport properties of the wiring units, the alkanedithiols.[23] A simple alkane wire has an even number of electrons per unit cell and thus is a band insulator. The Fermi energy E_F is placed inside the HOMO−LUMO gap (7.5 eV within present calculations); therefore, the zero bias conductance is nonvanishing only due to tunneling. The barrier height (Φ_A) is given by the separation of the alkane HOMO

(18) We mention that, in the case when nitrogen couples at "atop" or "hollow" position to a planar Au surface, we have $N_c \approx 5$. .8 (not shown in Figure 2). Such contact geometries were considered by many authors.[19–21] Our calculation for "atop" coupling shows that leakage rates remain largely invariant, and $\Gamma_L \simeq \Gamma_R \simeq \Gamma$ as one expects for strong coupling. We find a good quantitative agreement with refs 19 and 20. In our opinion, the quantitative mismatch with other authors[21] can be attributed at least partly to the limited number of Au atoms included or a relative low amount of *k*-points accounted for in their calculation setup.

(19) Pérez-Jiménez, A. J. *J. Chem. Phys. B* **2005**, *109*, 10052–10060.

(20) Stadler, R.; Thygesen, K. S.; Jacobsen, K. W. *Phys. Rev. B* **2005**, *72*, 2414014(R)

(21) (a) Wu, X.; Li, Q.; Huang, J.; Yang, J. *J. Chem. Phys.* **2005**, *123*, 184712-6. (b) Li, Z.-L.; Zou, B.; Wang, Ch.-K.; Luo, Y. *Phys. Rev. B* **2006**, *73*, 075326-7.

(E_{HOMO}) from the Au Fermi energy, $\Phi_A = E_F - E_{HOMO} = 2.2$ eV. The conductance through n -alkanedithiol junctions decays exponentially:[24] $G(n) = G_c \exp(-\beta_n n)$ with $\beta_n \propto \sqrt{\Phi_A d_0}$, where $d_0 = 1.28$ Å is a unit length of alkane chain, and G_c is a contact conductance. Calculations with the standard BP86 GGA-functional[13] give $\beta_n = 0.83$ per methylene group (see the Supporting Information for further details).

We are now in a position to analyze electron transport properties of the viologen derivatives (Figure 1a). We have imposed different oxidation states ($Q = +2$ or $+1$) at the redox center, which were compensated by a cylindrical grid of counter-(point)charges (gate) placed nearby the molecule (Figure 4a). These counter-charges model an electrochemical gate and ensure the charge neutrality of the whole system.[25]

Electronic structure calculations show that the bipyridinium core and the alkyl ligands are only weakly coupled: molecular orbitals (MOs) of the combined system are either localized at the viologen, very much resembling the 44BP wave functions, or form symmetric and antisymmetric combinations of the alkanes MOs (Figure 4d). In particular, the redox-active dication LUMO (Figure 4c) is localized at the viologen core. Therefore, the narrow LUMO-induced resonance is seen in the transmission spectrum $T(E)$ above the Fermi level (Figure 4b), similar to what we have observed for the 44BP (see Figure 2). However, in the case of viologen, the resonance width $\Gamma_n \propto \exp(-\beta_n n)$ is strongly reduced, reflecting the exponentially small tunneling probability through the alkyl wire of length n. The situation resembles a quantum dot weakly coupled to external reservoirs.

When the redox-active state (E_{LUMO}) is being tuned to the Fermi level (a typical experimental case considered in refs 5, 7), to apply a small source-drain voltage $eV \geq 2(E_{LUMO} - E_F)$ is enough for E_{LUMO} to fall within the bias window. The current is then essentially given by Γ_n. In the weak coupling regime, an electron, tunneling through the alkyl spacer, spends a long time $\sim\hbar/\Gamma_n$ at the viologen. Because populating the same orbital with the second electron costs a lot of charging energy U ($\sim$0.45 eV, see Figure 5), only after the first electron tunnels off the viologen, the second electron can come in, as long as $U >$ eV ("Coulomb blockade"). Therefore, in the case of elastic, that is, phase coherent, transport the current is given by the area under the spin-split resonance, which is within the voltage window, $I(V) = (e/h)\int_{-eV/2}^{+eV/2} T(E)\, dE = (e/h)\pi\Gamma_n$.

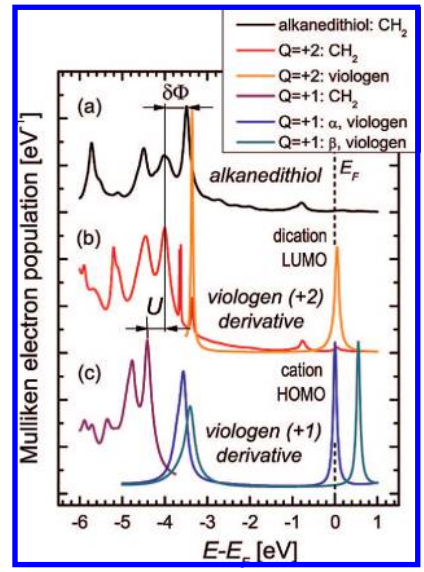

Figure 5. Mulliken electron population of molecular orbitals of the "extended molecule", when projected to different functional groups:[27] CH_2 or viologen. (a) $n = 4$ alkanedithiol; (b and c) $n = 4$ dithiolalkyl-viologens (see Figure 1a) with oxidation states $Q = +2$ (V^{2+}) or $+1$ ($V^{+\bullet}$) of the redox core, respectively. With the viologen [V^{2+}, plot (b)], the alkane levels are shifted $\delta\Phi \simeq 0.53$ eV downward in energy (see text for details), while the dication LUMO state, localized at the redox center, approaches the Fermi level. Note that the energy of this state with respect to alkane levels (which is the tunneling barrier seen by an electron) is underestimated by an amount of the charging energy $U \simeq 0.45$ eV, due to a well-known artifact of local density approximation.[28] U can be estimated from plot (c), where the V^{2+} dication LUMO evolves in the $V^{+\bullet}$ cation HOMO (here viologen electronic states, α and β, become spin split).

Now, also consider inelastic transport, which is described as a sequence of incoherent hops of single electrons on and off the molecule. The overall resistance R_{tot} of the junction, $R_{tot} \simeq R_L + R_R$, is then approximately the sum of two resistances of individual scatters (alkyl spacers) connected in series, with $R_L, R_R \propto \exp(\beta_n n)$. If the tunneling probability is small as compared to the voltage, $\Gamma_n \ll$ eV, we see that also sequential tunneling leads to the current of the form $I(V) \propto (e/h)\Gamma_n$. The prefactor includes the phonon specific physics, such as phonon-assisted tunneling.[26] We emphasize that both transport regimes, elastic and inelastic, have in common that $I(V) \propto \Gamma_n$; therefore, the exponential signature should be well observable.

We now proceed with the quantitative analysis. In Figure 4e, we plot the tunneling rate Γ_n over the number $N = 2n$ of CH_2 groups in the functionalized molecular wire. The calculations for the viologen dication state V^{2+} give for the decay constant a value $\bar{\beta}_{2n}^{00} = 0.66$, considerably larger than the asymptotic value $\beta_n/2 \approx 0.42$ being expected from a decay constant found for alkanedithiols (see Supporting Information). The distortion of the "shape" of the effective potential barrier due to a bipyri-

(22) We have to point out that quite generally calculated conductance values should be considered with caution, because the approximative character of the LDA-type functionals (that usually are the only available choice for such calculations) implies modifications in position and width of the LUMO peak in the transmission spectrum. Nevertheless, the overall structure of molecular orbitals is very well described within density function theory (DFT) even when local functionals are employed, ensuring the qualitative validity of our results.

(23) Li, Ch.; Pobelov, I.; Wandlowski, Th.; Bagrets, A.; Arnold, A.; Evers, F. *J. Am. Chem. Soc.* **2008**, *130*, 318–326.

(24) Prodan, E.; Car, R. *Phys. Rev. B* **2007**, *76*, 115102–15.

(25) We used the following parameters to construct cylindrical gates: a radius was chosen around $\sim$11 au with about $\sim$200 points forming a uniformly dense grid; to simulate screening effects due to solvent, a Gaussian distribution $q(z) \approx \exp[-(z - z_0)^2/2\sigma^2]$ of negative point charges was assumed as a function of their position around a center z_0 of the redox-active core, which carries the positive charge (here z-axis is along the gate), with $\sigma \simeq d_{N-N}/2 \simeq 3.33$ au being one-half of the core size.

(26) See, for example: (a) Lundin, U.; McKenzie, R. H. *Phys. Rev. B* **2002**, *66*, 075303-8. (b) Koch, J.; von Oppen, F. *Phys. Rev. B* **2005**, *72*, 113308-4.

(27) We used Mulliken analysis to find population weights by projecting molecular orbitals (MO) of the "extended molecule" on the basis functions of all atoms inside the given functional group. The curves in Figure 5 were obtained by summing Lorentzians centered at the MO energies and weighted with the Mulliken population numbers. We have ascertained in test calculations that a moderate rearrangement of point counter-charges (e.g., up to 15% change of the cylindrical gate radius, see ref 24) leaves our results almost invariant: peaks shift typically by no more than 0.1 eV. Because the potential barrier seen by electron is around $\sim$3.0 eV, such small shifts could lead to minor changes (up to $\sim$1.5% only) in the tunneling exponent β_{2n}.

(28) Köntopp, M.; Burke, K.; Evers, F. *Phys. Rev. B* **2006**, *73*, 121403-4(R)

(29) Note that the situation is very different in case of metallic systems, with conductance plateaus at $G \approx 2e^2/h$, where DFT-based transport calculations can be quantitatively very accurate.

dinium unit could explain part of the difference between these two values. In addition, we observe in Figure 5 an overall shift $\delta\Phi \simeq 0.53$ eV of the alkane-derived states downward in energy with respect to the Fermi level. That is because the alkane linkers feel the electrostatic potential of two holes localized at the viologen moiety, which is only partially screened by the gate. The shift gives rise to a somewhat higher tunneling barrier $\Phi_B = \Phi_A + \delta\Phi = 2.73$ eV (as compared to $\Phi_A = 2.2$ eV found for alkanedithiols) and, hence, to a larger exponent β_{2n}^0.

Also, it is likely that the calculated value $\bar{\beta}_{2n}^0 = 0.66$ is a lower limit to the true value. Because of the lack of the derivative discontinuity and other approximations, the GGA estimate of the dication (V^{2+})-derived LUMO energy is only approximate.[28] Its true position is higher by an amount of the charging energy U, which is the difference between the Kohn−Sham occupied level (α-HOMO of the radical cation $V^{+\bullet}$) and the unoccupied one (LUMO of the viologen dication V^{2+}). Performing calculations for the cation state, we estimate $U \simeq 0.45$ eV, which follows from the mutual off-set of the alkane derived states (see Figure 5) for different oxidation states, because both the cation-HOMO and the dication-LUMO are pinned to the Fermi level. We now can correct the effective tunnel barrier for this effect, $\Phi_B \rightarrow \Phi_B + U$, and thus obtain a modified exponent $\bar{\beta}_{2n} \approx \bar{\beta}_{2n}^0\sqrt{((\Phi_B + U)/\Phi_B)} = 0.71$.

Relation to Experiment

Regarding 44BP, we mention that a typical conductance $1.9 \times 10^{-2}G_0$ found in case of a large coordination number for the Au adatoms coupled to nitrogens (Figure 2a) is comparable to the result $\sim 0.01G_0$ reported by Xu and Tao.[4] Values close to this experimental one were obtained in previous first-principle studies.[19,20] These pointed out the sensitivity of the calculated conductaces to the contact geometry, arguing that a proper choice of metal–molecule binding would lead to a perfect agreement between calculations and experimental findings. However, this statement is to be taken with a grain of salt. As was emphasized above, absolute theoretical values should be considered with caution because of approximations inherent to the available density functionals. Therefore, a precise quantitative agreement of transport coefficients with the experimental results is not expected and should probably be considered accidental, if observed.[29] We find more intriguing a qualitative theoretical prediction that a broad spectrum of conductance values spreading 2 orders of magnitude might be observed, if perhaps a scrupulous analysis of carefully recorded histograms in the low conductance regime is performed. Whether or not an observation of a distinct peak series indicating the smaller conductances is experimentally feasible depends on the statistical weights of different contact geometries and their ability to resist the destruction under the current flow. While predicting absolute conductance values (i.e., prefactors) is difficult, to compare relative trends may be beneficial. For example, in the case of dithiolalkyl-viologens, we find the theoretical decay constant, $\bar{\beta}_{2n} = 0.71$, to match well the experimental one, $\beta_{2n}^{exp} \approx 0.75$, reported by Li et al.[7] (see inset in Figure 4e).

Finally, we discuss the origin of "conductance switching" observed experimentally for electrochemically gated viologen derivatives[5,7] (see Introduction). Our calculations suggest (see Figure 4e) that under experimental conditions the LUMO-transport resonance (Figure 4b) lies well inside the bias window, thus $I(V) \propto (e/h)\Gamma_n$. If the resonance were outside this window, the current would be proportional to $\propto \Gamma_n^2/(E_{LUMO} - E_F)$ (off-resonance tunneling), implying exponent $2\bar{\beta}_{2n}$, which is twice the value that is actually observed. Therefore, a small shift of the resonance within the bias window, as it is induced by flipping from the titled into the planar conformation (see Figure 3 in the case of 44BP), cannot explain the observed difference in conductances. Moreover, we also found the direct effect of the torsion angle ($\theta = 0°$ for the $V^{+\bullet}$ vs $\theta = 42°$ for the V^{2+}) on the tunneling rate Γ_n to be negligible. Thus, our analysis does not give an indication that a gate-driven conformational change could explain the experimental switching effect all by itself.

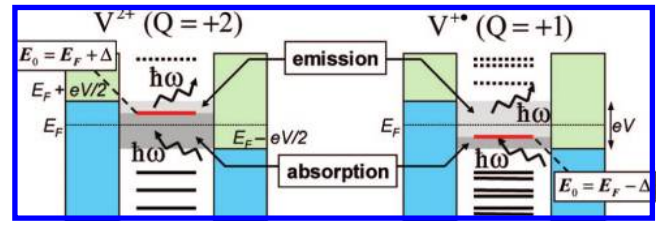

Figure 6. Phonon-assisted tunneling through the redox level E_0 of a viologen under finite bias $eV > 2\Delta$: in case of the reduced cation $V^{+\bullet}$ state ($E_0 = E_F - \Delta$, right panel), a wider energy window (shown in light gray) is available for an electron to emit phonons and reach the resonant level E_0 as compared to the dication V^{2+} state ($E_0 = E_F + \Delta$, left panel), leading to a larger conductance.

Instead, we propose that switching could arise from inelastic constituents of tunneling through the redox level E_0 localized at the viologen core. The tunneling electron interacts with molecular vibrations, thus losing or acquiring energy. Phonon satellites[26] appear in the transmission spectrum $T(E)$, indicating opening of new, inelastic resonant channels with energies above and below E_0. Imagine the unpopulated electronic level E_0 (LUMO) of the dication, V^{2+}, to be placed a small energy, Δ, above E_F (see Figure 6, left panel). With increasing gate voltage this level can be shifted downward in energy, so that its average occupation number increases gradually. Once this number is close to unity, say at an energy $\sim\Delta$ below E_F, then the level is essentially the cation, $V^{+\bullet}$, HOMO (Figure 6, right panel). Now, when a large enough source-drain bias, say $eV > 2\Delta$, is switched on (Figure 6, gray zone), the viologen level E_0 always falls into the bias window and current will flow. However, for the cation state $V^{+\bullet}$, the phase space for the phonon emission typically exceeds the one for the absorption. In other words, the energy window for emitting phonons, $E_0 < E < E_0 + (eV/2 + \Delta)$ (Figure 6, right, light gray zone), is much bigger than the one for absorption, $E_0 - (eV/2 - \Delta) < E < E_0$ (Figure 6, right, dark gray zone). For the dication state V^{2+}, the picture is just the opposite (Figure 6, left). Because at $k_BT \ll eV$, it is easier to emit phonons rather than absorb them, the overall inelastic contribution to the current is expected to be larger for the "reduced" cation state $V^{+\bullet}$ of the viologen, consistent with experimental findings.[5,7] The observed saturation of the conductance, away from the reversible redox transition controlled by the electrochemical gate,[7] might indicate the regime when the redox level E_0 is being pulled out of the bias window. The proposed mechanism relies on the assumption for the phonon spectrum to be quite broad as compared to the bias: $\hbar\omega_{max} > eV$ (here ω_{max} is the highest viologen's phonon frequency involving C−C bonds). Our preliminary estimates are not inconsistent with this requirement, because for the viologen $\hbar\omega_{max} \approx 0.2$ eV, while a typical bias energy is only ~ 0.1 eV.

To summarize, the LUMO drives the single molecule conduction of the 4,4′-bipyridine (44BP). We predict that its transmission can differ by orders of magnitude; the contact

geometry plays a crucial role. In this respect, the N−Au coupling is vastly different from the S−Au bond, where the latter accounts only for a moderate factor of ∼4 in conductance of thiol-modified molecules, like alkanedithiols.[23] We have shown as well that the transport properties of the dithiolalkyl-viologens are governed by the redox-active level localized at the bipyridinium core. The resonant transmission through this state determines the tunneling exponent of the conductance, observed experimentally. A value $\beta_{2n} = 0.71$ was calculated in close agreement with data of ref 7. We proposed that inelastic processes, arising from the interaction of a tunneling electron with molecular vibrations, could be the origin of conductance switching observed in recent experiments.[5,7]

Acknowledgment. We would like to thank I. Pobelov, Ch. Li, V. Meded, Ch. Rajadurai, F. Schramm, M. Ruben, M. Mayor, O. Rubner, and F. Weigend for fruitful discussions. We are especially grateful to Th. Wandlowski for introducing us with patience into the field of electrochemically gated single molecule transport measurements, which partly initiated the scientific work reported in this Article. Also, we thank M. Mayor, I. Pobelov, and Th. Wandlowski for their constructive collaboration in the framework of the Kooperationsprojekt der Helmholtzzentren Karlsruhe and Jülich "Integrated Molecular Switches". Additional financial support through the DFG "Center of Functional Nanostructures" situated at the University of Karlsruhe is gratefully acknowledged.

Supporting Information Available: Electron transport properties of alkanedithiol wires. This material is available free of charge via the Internet at http://pubs.acs.org.

JA800459K